China Geology 6 (2023) 594−610

China Geology

Journal homepage: http://chinageology.cgs.cn
https://www.sciencedirect.com/journal/china-geology

Biophysical warming patterns of an open-top chamber and its short-term influence on a *Phragmites* wetland ecosystem in China

Xue-yang Yu[a, b], Si-yuan Ye[a, b,*], Li-xin Pei[a, b], Liu-juan Xie[a, b], Ken W. Krauss[c], Samantha K. Chapman[d], Hans Brix[e]

[a] *Key Laboratory of Coastal Wetland Biogeosciences*, *Qingdao Institute of Marine Geology*, *China Geological Survey*, *Ministry of Natural Resources*, *Qingdao* 266071, *China*
[b] *Institute of Marine Science and Technology*, *Shandong University*, *Qingdao* 266237, *China*
[c] *Wetland and Aquatic Research Center*, *U.S. Geological Survey*, *Lafayette* 70506, *United States of America*
[d] *Department of Biology*, *Villanova University*, *Villanova* 19085, *United States of America*
[e] *Department of Biology*, *Aarhus University*, *Aarhus* 8000*C*, *Denmark*

ARTICLE INFO

Article history:
Received 19 May 2021
Received in revised form 1 September 2021
Accepted 8 April 2022
Available online 29 January 2023

Keywords:
Open-top chambers (OTCs) warming
Phragmites australis wetland
Short-term ecosystem impact
Climate warming
Soil heat flux
Soil-atmosphere heat transfer
Ecological geological engineering
Hydrogeological engineering
Yellow River Delta

ABSTRACT

Passive-warming, open-top chambers (OTCs) are widely applied for studying the effects of future climate warming on coastal wetlands. In this study, a set of six OTCs were established at a *Phragmites* wetland located in the Yellow River Delta of Dongying City, China. With data collected through online transmission and *in-situ* sensors, the attributes and patterns of realized OTCs warming are demonstrated. The authors also quantified the preliminary influence of experimental chamber warming on plant traits. OTCs produced an elevated average air temperature of 0.8°C (relative to controls) during the growing season (June to October) of 2018, and soil temperatures actually decreased by 0.54°C at a depth of 5 cm and 0.46°C at a depth of 30 cm in the OTCs. Variations in diel patterns of warming depend greatly on the heat sources of incoming radiation in the daytime versus soil heat flux at night. Warming effects were often larger during instantaneous analyses and influenced OTCs air temperatures from −2.5°C to 8.3°C dependent on various meteorological conditions at any given time, ranging from cooling influences from vertical heat exchange and vegetation to radiation-associated warming. Night-time temperature depressions in the OTCs were due to the low turbulence inside OTCs and changes in surface soil-atmosphere heat transfer. Plant shoot density, basal diameter, and biomass of *Phragmites* decreased by 23.2%, 6.3%, and 34.0%, respectively, under experimental warming versus controls, and plant height increased by 4.3%, reflecting less carbon allocation to stem structures as plants in the OTCs experienced simultaneous wind buffering. While these passive-warming OTCs created the desired warming effects both to the atmosphere and soils, pest damages on the plant leaves and lodging within the OTCs were extensive and serious, creating the need to consider control options for these chambers and the replicated OTCs studies underway in other Chinese *Phragmites* marshes (Panjin and Yancheng).

1. Introduction

Current global temperatures have increased by an average of 1ºC compared with pre-industrial levels (Hawkins E et al., 2017), and modelling predicts that warming of 1.5ºC may occur by 2030 relative to pre-industrial levels (IPCC, 2013, 2022). Research efforts have been focused on understanding not only the influence that small increments in atmospheric warming might have on coastal wetlands over decadal times scales, but also how acute increases in temperatures associated with year-to-year variability in warming might influence coastal plant communities and processes, particularly those associated with carbon, nutrient, and water cycling.

Coastal wetlands perform a variety of ecosystem services, including flood protection; erosion control; provision of food and habitat for wildlife, including commercially and recreationally important fish; regulation of water quality; recreation; and carbon sequestration. These ecosystem services have been estimated to be worth billions of dollars

First author: *E-mail address*: yuxueyang@caas.cn (Xue-yang Yu).

* Corresponding author: *E-mail address*: siyuanye@hotmail.com (Si-yuan Ye).

Literary editor: Li-qiong Jia
doi:10.31035/cg2022064
2096-5192/© 2023 China Geology Editorial Office.

(USD) globally (Perillo GME et al., 2009). Projected increases in temperature, particularly at high latitudes, will likely alter the rates of chemical reactions and biogeochemical processes in plants and soil, and shift the seasonal cycles of production and consumption of organic matter in ways that may dramatically change these ecosystem services qualitatively and quantitatively (Körner C and Basler D, 2010; Rouse WR et al., 1992). The anticipated direct effects of temperature increases include stimulation of respiration (Bondlamberty B and Thomson A, 2010), photosynthesis (Rätsep M et al., 2018), methanogenesis, and methane oxidation (King G and Adamsen A, 1992; Macdonald JA et al., 1998), as well as changes in the solubility of these gases. Other impacts of warming could include shifts in the outcome of competition between species. and increases in the duration of the summer growing season which alters plant carbon balance.

Wetland plant responses to these changes can be obtained from examining wetlands across natural climatic gradients, from the tropics to high latitudes (Mozdzer TJ and Caplan JS, 2018), and from examining the geological record throughout past glacial-interglacial cycles (Liu J et al., 2018). More direct investigations of wetland plant responses to warming can be gained by implementing controlled experiments in which environmental variables are manipulated one at a time or in combination (Crowther TW et al., 2016; Deegan LA et al., 2012). However, due to spatial and temporal differences among wetland ecosystems and how they function (Xu YY and Ramanathan V, 2012; Ye SY et al., 2016), there is insufficient evidence to explain the impact of climate change, such as warming, on many wetland ecosystems (Meng L et al., 2016), prompting increasingly more attention on experimental studies from specific wetland ecosystems and less reliance on modeling generalities. Therefore, temperature control experiments have been widely used to address the broad range and complexity that must be considered in projecting the response of coastal wetlands to global warming (Crowther TW et al., 2016).

Passive warming methods, such as open-top chambers (OTCs), plastic tents, and infrared reflection boards, do not contain external heat sources and rely on passive energy and heating from solar irradiance. These warming methods are useful for working in remote natural ecosystems where power is unavailable (Aronson EL et al., 2009; Zhu JT et al., 2017). Further, passive warming provides a more natural context for simulating atmospheric warming and how that may resonate with soil warming. However, these passive warming experiments often suffer from the limited magnitude of warming influences created experimentally, especially from the transmission of warming to soils (Carey JC et al., 2018). Active warming methods, such as the use of heating coils and infrared lights, are often more deliberate in attaining larger differences in warming at the desired locations, but these are also more energy-consuming and difficult to implement without line power (Marion GM et al., 1997), Further, active warming experiments often impose variability in the warming process that is unnatural and can also cause artificially low soil moistures due to their induction of soil water evaporation. Using a novel design of passive warming chambers, we aim to explore whether passive warming can induce soil warming.

Hexagonal OTCs are widely used in the arctic tundra, with the height of the OTCs typically positioned slightly higher than the vegetation canopy in those environments (ca. 30–60 cm tall). Generally, the amount of warming (hereafter, “warming amount”) of the internal air volume in arctic OTCs ranges from 0.3–6.0°C but results show high variability in warming amounts registered across a range of study sites and slight differences in design (Edith B et al., 2013; Romero-Olivares AL et al., 2017). Wang JF and Wu QB, 2013 established two kinds of warming chambers with heights of either 40 cm or 80 cm in a short-vegetation meadow environment of the Qinghai-Tibet Plateau. Atmospheric temperature enhancement reached 5.29°C and 1.84°C, respectively, in 80 cm high and 40 cm high chambers. This experimental warming amount is higher than from OTCs deployed in even higher latitudes such as Antarctica where OTCs warming was less effective (0.1–1.6°C) (Marion GM et al., 1997), though absolute amounts of warming expected to influence a specific location in the future are relative and latitude specific. Moreover, the warming amount of a heating box (50 cm high with a base area of 1.24 m^2) installed in Germany was 0.4–1.5°C (Cornelius C et al., 2015), and a 9-year field OTCs warming experiment in Sweden showed a warming amount of 0.2–1.0°C. A meta-analysis from northern Europe and the United States showed that the warming range from multiple passive warming stations was 0.3–6.0°C (Rustad LE et al., 2001), suggesting that experimental approaches can theoretically simulate projected atmospheric warming conditions over the next century.

The warming patterns of OTCs strongly depend on their structure and design. Generally, the greater extent of top closure for OTCs leads to a greater warming amount because of a higher temperature difference between inside and outside the chamber from more limited heat escape. The warming amount under full sunlight is often better than in cloudy and rainy periods, with the warming amount from full sunlight periods able to reach as high as 16.4°C in some environments during instantaneous measurements (Wookey PA et al., 1993).

The warming amount of air temperature is generally higher than soil temperature, and warming amounts often decrease with depth into the soil. For example, surface soil temperature was elevated experimentally by 1.8°C according to some field observations (Sun SQ et al., 2013). Along with temperature differences, OTCs often influence the relative humidity of the air. Sun SQ et al., 2013 observed a 6.1% relative humidity drop inside an OTCs versus outside. This is believed to be related to higher evaporation, stimulated plant transpiration, and subsequent soil dehydration inside the OTCs from that location on the Qinghai-Tibet Plateau, causing a loss of soil moisture content of 2.8%–3.8% (Wang JF and Wu QB, 2013). In a past study, experimental warming

was shown to increase ecosystem respiration (Chen J et al., 2016), promote above-ground biomass (Baldwin AH and Jensen K, 2014; Day TA et al., 2010), accelerate the mineralization of organic matter (Li JW et al., 2015), and stimulate greenhouse gas release (Grogan P and Chapin III FS, 2000; Zhou YM et al., 2016). As a result, it is reasonable to expect that a new balance of carbon, water, and nutrient cycling will be established under future warming scenarios for coastal wetlands (Hobbie SE and Chapin III FS, 1998). Plant phenology, soil microbial composition, and plant community structure will also become altered with the successional process stimulated by warming (Zhang ZS et al., 2017). However, it is important to note that some studies have suggested that the impact of warming on ecosystems might not be that significant (Fu G et al., 2013). Most OTCs are established mainly in northern latitudes and are within meadows or low shrub ecosystems. Yet, there is still a lack of acknowledgment as to how large vascular plants might react to future warming conditions.

To explore the warming influence on a reed (*Phragmites australis*) wetland system, field sites were established and an OTCs design capable of warming vegetation heights up to 2.5 m was implemented, which was part of the Coastal-wetland Research On Warming Network (CROWN) project. This project presents the warming patterns generated from the novel coastal wetland OTCs design and shows how this novel design can be used to generate soil warming. This project also demonstrates how radiation and wind speed influence experimental warming on ecosystem variables and short-term plant traits are also quantified and described. The project also identifies several important artifacts that need to be sorted out as additional large OTCs designs are implemented, and hope to stimulate new discourse on realities associated with OTCs designs.

2. Materials and methods

2.1. Study site

The study site is in the modern Yellow River Delta, which is in Kenli District, just outside of Dongying City of Shandong Province, China. In 1976, the mouth of the Yellow River and its associated wetlands were determined by a water conservancy project in the estuary to be rather critical for preservation and has become the focus of numerous wetland and wildlife studies since. The Yellow River Delta has a temperate monsoon climate with annual precipitation of 530–630 mm and an average annual temperature of 13.3°C (Yu JB et al., 2014). The Delta depends greatly on the water supply of the Yellow River as the annual evaporation is as high as 1900–2400 mm (Yu JB et al., 2014), which is only partly supplied by local rainfall. In most parts of the Delta, surface elevation is lower than 10 m (A.S.L.), and is flat with a slope of less than 0.1%. The soil type is gley saline soil according to the standard of the United Nations Food and Agriculture Organization (FAO). The soil texture is sandy loam and the dominant vegetation of the Delta's wetlands and adjacent levees include the common reed (*Phragmites australis*), alkaline tamarisk (*Tamarix chinensis*), and seablite (*Suaeda salsa*) (Yu JB et al., 2014).

The content of organic carbon, total nitrogen, and sulfur of Yellow River Delta soils was 0.4–8.5 mg C/g, 98.1–762. 7 mg N/g, and 92.0–329.5 g S/g, respectively (Ding YR et al., 2012). Surface (0–20 cm) soil bulk density was 0.86–1.17 g/cm^3 according to Yu JB et al., 2014, but it could also be as high as 1.55–1.97 g/cm^3, and the soil carbon ratio is about 50 (Ding YR et al., 2012).

In this study, the OTCs are located at 37º45′51″N and 119º00′59″E, or 30 km west of the Yellow River mouth and 3 km to the south of the main river channel (Fig. 1). There is no direct connection between the OTCs field site and the main river channel; however, seasonal high water from overbank flooding or groundwater discharge can periodically spill into the site. The average height of reed vegetation is approximately 1.8 m.

2.2. OTCs design

The OTCs were designed as octagonal prisms to promote rigidity, and they were constructed to a height of 2.7 m, each covering an area of 5.54 m^2; in a sense, these are mini-greenhouses. The eight sides are 1.07 m wide each, and they are interlocked with aluminum alloy frames. The sides were made of 4 mm thick stalinite glasses, and are clear and transparent (with 92% transmittance), allowing them to maintain incoming solar radiation flux to promote heating and not influence photosynthetic activity. Each OTC was fixed at eight base plates associated with side junctions, and the plates were attached to stable poles inserted 1.5 m into the soil. There was a 10 cm space between the bottom of the OTCs and the soil surface to allow natural water exchange below the OTCs. Six OTCs were erected in the early spring of 2018, and each OTC had frail netting draped over the top to prevent small birds from entering the OTCs and becoming trapped. Otherwise, they were fully open-topped.

There is a control plot adjacent to each OTC. The control plots were characterized by frames of polyvinyl chloride (PVC), and were exacting to the OTCs dimensions but without stalinite glass and metal frames. Boardwalks were built among and around each OTC and control site to avoid stepping on the soil surface during OTCs maintenance, sensor establishment and downloading, and experimental measurements. Each OTC and paired control plot were replicated six times.

2.3. Automated meteorological station

An automated meteorological station was installed on one of the six OTCs. Several sensors and installation positions were established (Table 1). The system was powered by lead acid batteries, charged by solar panels connected to a voltage regulator system. Raw data were sampled at 2-minute intervals and summarized at 10-minute intervals. Missing values of meteorological data were filled by linear

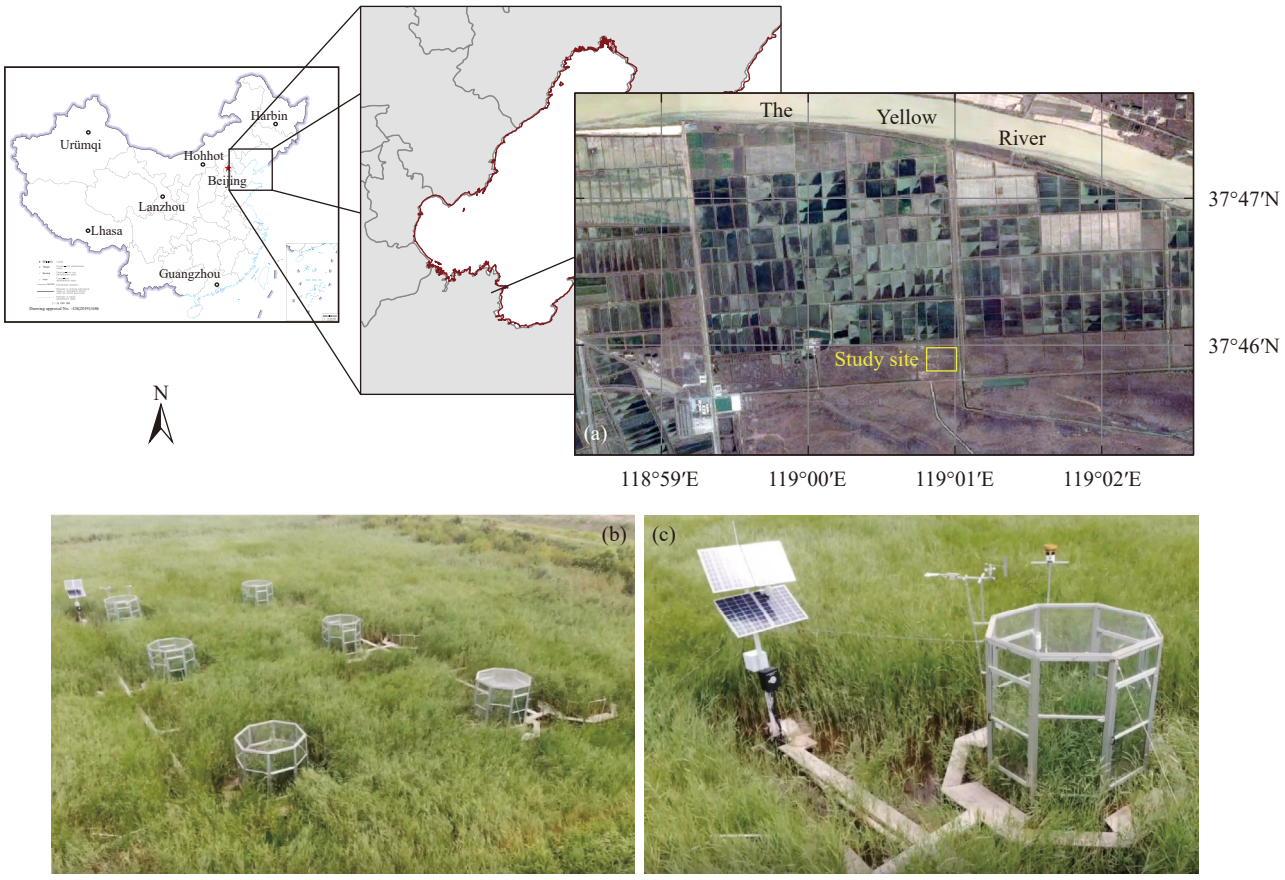

Fig. 1. Location (a) of the warming experiment and open-top chamber (OTC) chamber setup (b, c).

Table 1. Details of the automated environmental data collecting system, including the number of sensors and location of each sensor type.

Items	Manufacturer	Model	Numbers	Installation position
Data logger	Campbell Scientific, Inc., U.S.	CR1000	1	1.5 m above soil surface on the solar panel pole, outside OTCs
Soil temperature sensor	Campbell Scientific, Inc., U.S.	CS655-L	8	5 cm, 10 cm, 20 cm, and 30 cm below the soil surface each inside OTC and in the control plot
Temperature & RH probe	Vaisala, Finland	HMP155A	4	100 cm, 190 cm above the soil surface each inside OTCs and in the control plot
Radiation shield	Vaisala, Finland	41005-5	4	Same as previous
Quantum sensor	Li-Cor Environmental, Inc., U.S.	LI190R	1	3.2 m above the soil surface, outside OTCs
Precipitation gauge	Campbell Scientific, Inc., U.S.	TB4MM-L	1	3.2 m above the soil surface, outside OTCs
Soil heat flux plate	Campbell Scientific, Inc., U.S.	HFP01SC-L	4	5 cm, 15 cm below the soil surface each inside OTCs and in the control plot
Net radiometer	KIPP & ZONES, The Netherlands	CNR4	1	3.2 m above the soil surface, outside OTCs
Wind sensor	MetOne Instruments, Inc., U.S.	034B	1	3.2 m above the soil surface, outside OTCs
Water level sensor	Campbell Scientific, Inc., U.S.	CS456	1	In well, 1.2 m below the soil surface, outside OTCs
Barometer	Campbell Scientific, Inc., U.S.	CS100	1	In waterproof box holding CR1000, vented outside with tube

interpolation when functionally reasonable.

2.4. Plant investigation

Plants were measured from all six OTCs and control plots in mid-October when plant biomass reached a seasonal peak. Three subsample locations were randomly chosen within each OTC and control plot by using a frame to mark an area of 0.25 m^2 (0.5 m × 0.5 m). Within each frame (n=3 per OTC or control plot), basal stem diameters were recorded at the soil

surface by a vernier caliper to an accuracy of 0.01 mm. At the same time, the height of each plant up to the first level leaf top was recorded by a long ruler pole to an accuracy of 0.1 cm. To avoid disturbing the experimental units, the biomass of plants was estimated using an empirical equation determined *in-situ*. To determine the localized empirical equation for plant biomass estimation, 25 shoots of randomly chosen reeds were clipped at the soil surface from outside the experimental units (OTC or control) after they were first diameter and height measured. The fresh weight of each shoot was weighed by a scale (with an accuracy of 0.01 g), and the plants were put into a 65°C convection oven until the weight was constant (more than 24 hours). The dry weight of each shoot was then re-weighed on the same scale, and a relationship was developed among plant height, basal diameter, and dry biomass to apply non-destructively to OTCs and control plot responses. The water content of the reed plant was also estimated according to the ratio of dry weight and fresh weight. The investigated fresh weight was estimated by a logistic form equation from Yu XY and Ye SY, 2020 (Equation 1):

$$W = \frac{w_1}{1+e^{-a(H-b)}} + \frac{w_2}{1+e^{-c(D-d)}} \quad (1)$$

Where least squares fitting parameters, H and D represent the height (in cm) and basal stem diameters (in mm) of a reed shoot, and W is the estimated plant biomass (in gram). The fitting parameter w_1 was 8.74 g, w_2 was 25.70 g, a was 0.14 cm^{-1}, b was 200.44 cm, c was 0.97/mm, and d was 4.6 mm for the local Yellow River Delta reed (Fig. 2). The dry weights were attained through a water content correction of 0.542.

2.5. Data analysis

All the environmental data in this paper were collected from the experimental plots from 14 June to 30 November, 2018. Plant measurements were taken on 20–25 October. Significant differences among warming treatment parameters were evaluated using simple one-way ANOVA tests conducted using the SCI-py package on the Python 3.6 platform. The warming amount was evaluated by the difference between the temperature inside the OTCs versus outside the OTCs as matched pairs. Preliminary differences in plant height, basal diameter, and biomass of Phragmites plants were also determined with a one-way ANOVA. The deviations of the mean level were normally distributed, thus no data transformations were carried out.

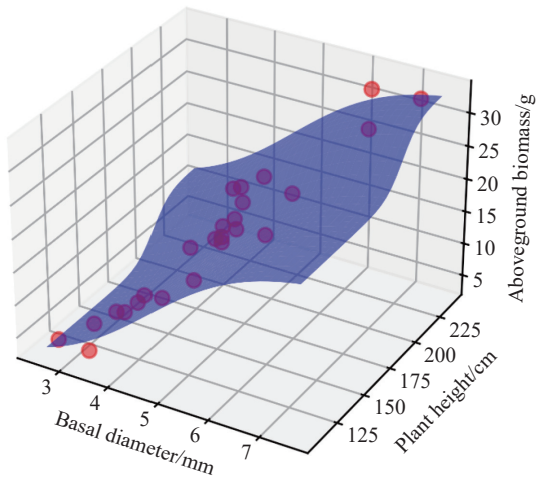

Fig. 2. Visualization of plant biomass (g fresh weight) estimation equation. The red dots indicate the measured 25 shoots of local *Phragmites*, and the integrated blue surface indicates the fitting equation for estimating plant fresh biomass.

3. Results

3.1. Site-level meteorology data

The maximum daily air temperature was 30.7°C which occurred on 7 August and decreased consistently from that date to a low of approximately 10°C by late October (Fig. 3). The seasonal average air temperature was 22.1°C and the monthly average air temperature of June, July, August, September, and October was 24.4°C, 27.2°C, 26.7°C, 20.7°C, and 13.3°C, respectively. The precipitation during the observation period was 252.9 mm, with a daily maximum precipitation event appearing on 14 August (71.5 mm; or 28% of the rainfall for the observational period). Indeed, there were four heavy precipitation events: 25 June (38.4 mm), 13–15 July (71.7 mm), 23–24 July (34.8 mm), and 13–15 August (88.4 mm). The amount of these heavy precipitation events combined was 233.3 mm which was equal to 92% of all recorded rainfall for the observational period.

Daily averaged net radiation varied from 19.7 W/m^2 to 197.5 W/m^2 and peaked at mid-day on 21 August (at 811.0 W/m^2). The net radiation varied seasonally and the average net radiation of June, July, August, September, and November was 149.2 W/m^2, 144.2 W/m^2, 137.6 W/m^2, 95.8 W/m^2, and 64.6 W/m^2, respectively. There was a significant difference in net radiation before and after August ($p<0.05$); however, no significant inter-monthly difference was noted in net radiation before or after August ($p>0.05$). Most daily wind speeds were lower than 3 m/s, and the highest daily wind speed appeared on 15 August when the heaviest single-day rainfall was also recorded. The water table varied from −62 cm to 45 cm relative to the soil surface (i.e., negative values refer to a water table below ground), since the 15 August heavy rain event, the water table kept rising and remained flooded until the end of the observation period. Water table maintenance at the soil surface depends on rainfall events, and slight drawdowns below the soil surface between June and August coincided with an approximate 10–15 days lag between the last rainfall event and apparent water drawdown below the soil surface as ET overcame the surface (or groundwater) water balance provided by individual rainfall events.

3.2. Diel and seasonal variation of OTCs warming amount

During the displayed days, no significant difference was detected between the upper level and the lower level except for the noon period of 18 June (Fig. 4). However, the

warming amount of the OTCs on sunny days is certain during these days. For the upper level, the daytime (6:00–18:00) average OTCs warming amount on 18 June, 3 August, and 27 September was 0.76°C, 3.89°C, and 1.38°C, respectively, but the instantaneous warming amount could be as high as 1.96°C, 7.90°C, and 5.32°C for the same three days (Fig. 5), respectively. Night-time air cooling of OTCs happened occasionally (Fig. 5).

The diel variation of soil temperature was unimodal on 18 June and 3 August but differed slightly from this pattern in the late autumn (27 September). Unlike air temperature warming patterns, soil temperature warming amount was more stable over a day with major depression (Fig. 4). The average daily warming amount of the full soil profile from 5

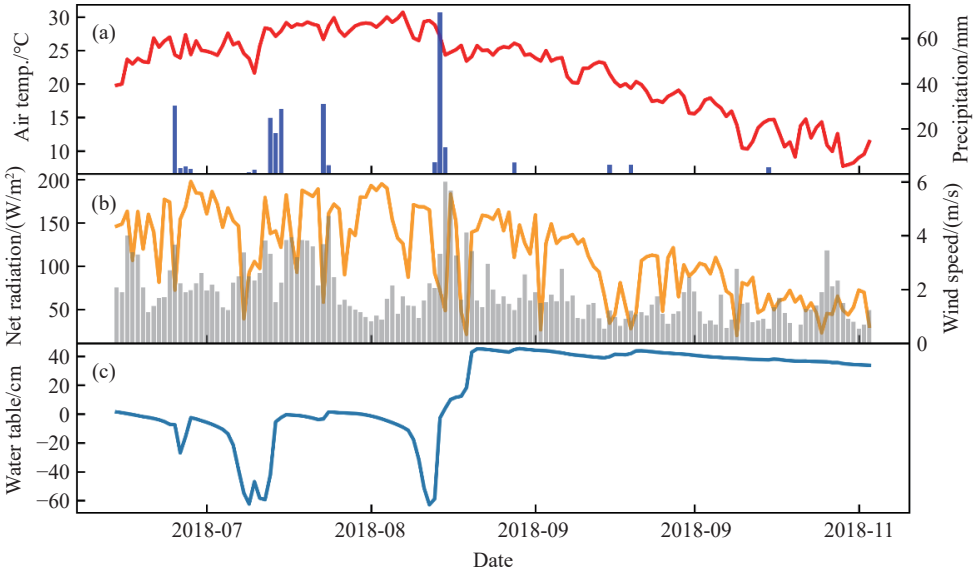

Fig. 3. Daily averaged environmental variables associated with OTCs and control plots in the Yellow River Delta. a–red line represents the air temperature and the blue bars indicate precipitation; b–orange line represents the daily averaged net radiation and the grey bars represent the wind speed; c–water table relative to the soil surface during the observing period.

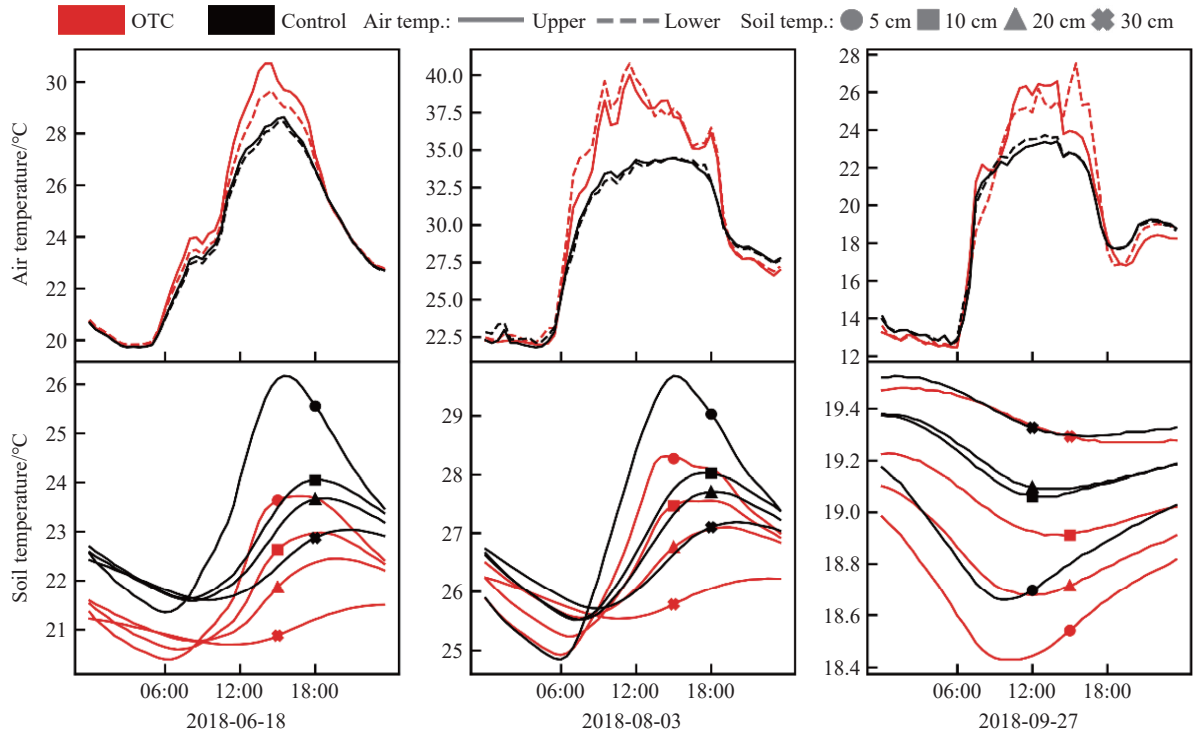

Fig. 4. Diel variation of air temperature and soil temperature on typical sunny days. Temperatures in OTCs are colored red and the temperatures in the control plots are colored black. For the air temperature graphs, the upper level (190 cm) temperatures were drawn with solid lines while the lower level (100 cm) temperatures were drawn with dashed lines. Soil temperatures of depth 5 cm, 10 cm, 20 cm, and 30 cm are marked with circles, squares, triangles, and crosses, respectively. Three typical days of full sunlight were selected including 18 June, 3 August, and 27 September, indicating late spring, summer, and autumn patterns.

cm to 30 cm on the three selected days was −1.20°C, −0.44°C, and −0.19°C, respectively. Soil warming amounts did not reach the magnitudes of air temperature warming amounts. Due to heat transfer processes, the timestamp of when soil temperature peaked was delayed by approximately 120 minutes from 5 cm to 30 cm depths.

The diel relationships for air temperatures on cloudy/rainy days were, however, not the same as for sunny days, when no air warming occurred. Even though, soil cooling still existed (Fig. 6). For instance, on 19 August, the air temperature was

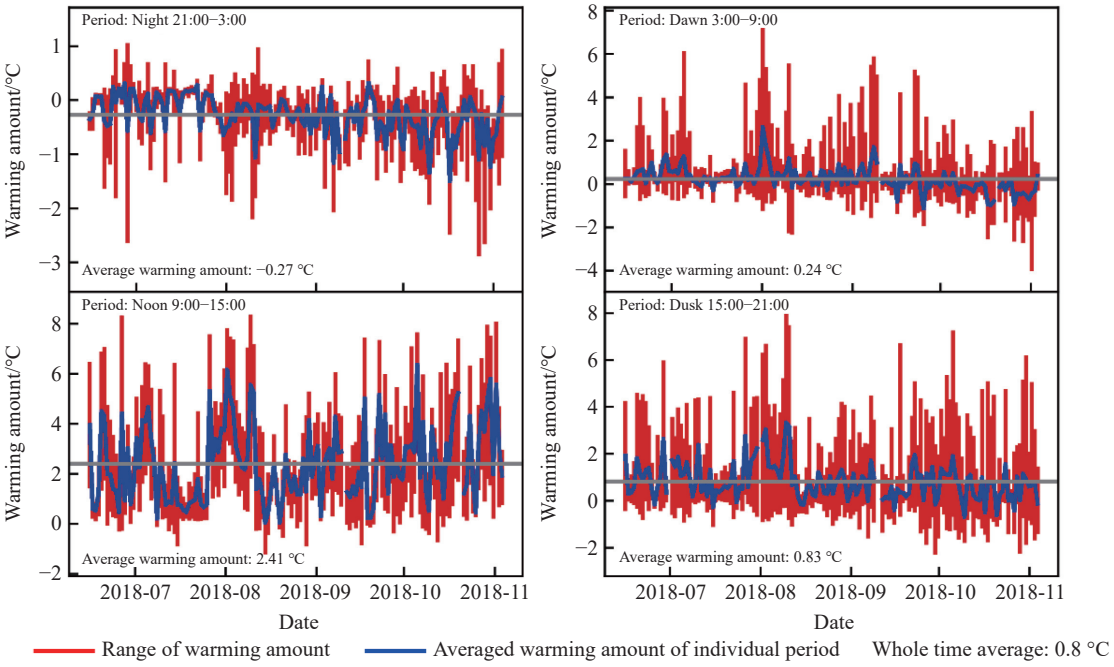

Fig. 5. OTCs warming amount of air temperatures over four diel periods. Periods were determined as night (21:00 to 3:00), morning (3:00 to 9:00), noon (9:00 to 15:00) and dawn (15:00 to 21:00). The red bars represent the warming amount range for a single day during a corresponding period. The blue lines represent the average warming amount of the corresponding period.

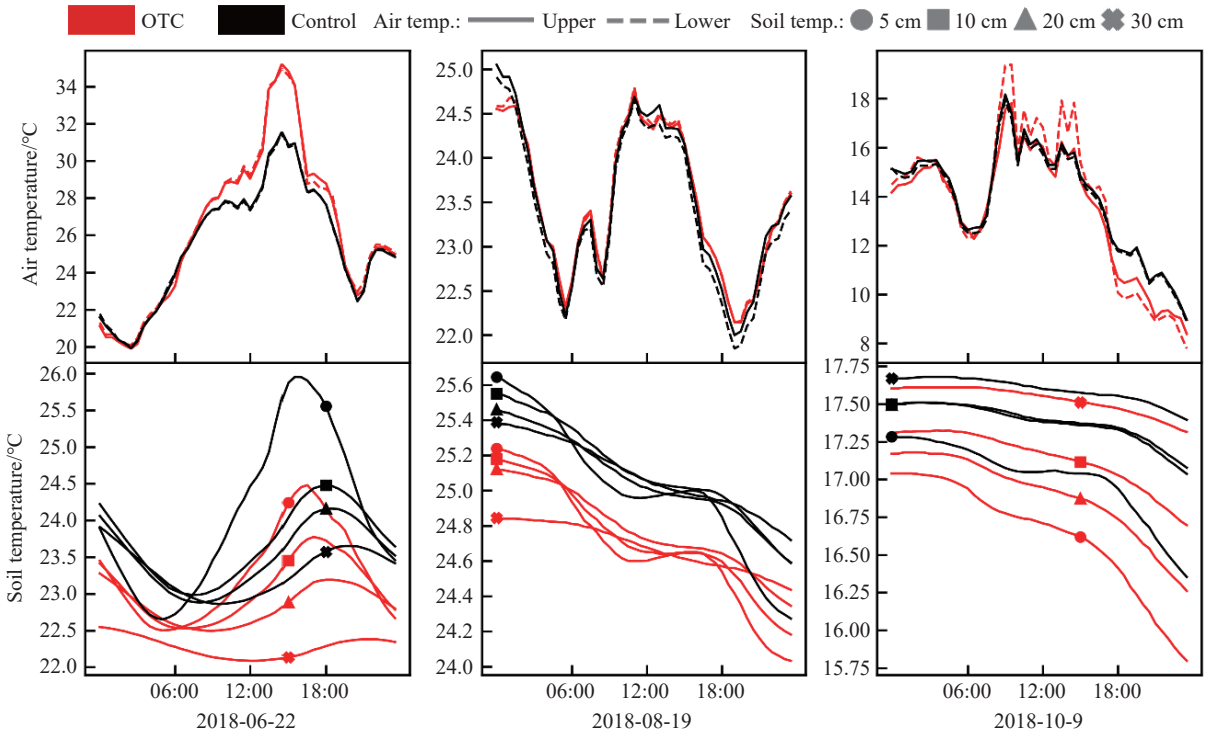

Fig. 6. Diel variation of air temperature and soil temperature on typical cloudy/rainy days. Temperatures in OTCs are colored red and the temperatures in the control plot are colored black. For the air temperature graphs, the upper level (190 cm) temperatures were drawn with solid lines while the lower level (100 cm) temperatures were drawn with dashed lines. Soil temperatures of depth 5 cm, 10 cm, 20 cm, and 30 cm are marked with circles, squares, triangles, and crosses, respectively. Three typical days of cloudy/rainy were chosen as 22 June, 19 August, and 9 October, indicating late spring, summer, and autumn patterns.

lower than the surface soil temperature all day long and the soil temperature kept decreasing. Under such conditions, the temperature inside the OTCs was still lower than outside. The daily average soil warming amount at 5 cm, 10 cm, 20 cm, and 30 cm was −0.33°C, −0.39°C, −0.29°C and −0.41°C, respectively, which was lower than for the sunny days (Fig. 6).

3.3. OTCs warming amount and diel cycles of change

Night-time air temperature depression occurred for more than 90% of the observing days, resulting in an average cooling amount of −0.27°C at night (Table 2; Fig. 5), as temperatures in the OTCs decreased significantly (and paradoxically) relative to the outside (controls). The mean air temperature warming occurred around mid-day, with an average warming amount of 2.41°C for the OTCs. Early morning (within 30 minutes of daybreak) and dawn warming amounts became weaker over diel cycles, and averaged 0.24°C and 0.83°C, respectively. The average air warming amount was 0.80°C in the OTCs during combined dawn and early morning observation periods. In comparison, the maximum air warming amount was 8.3°C in the afternoon (14:39) on 9 August, indicating that warming amounts can be impressive with this OTCs design, but not sustained. Compared with air warming, the soil warming amount was relatively lower with an average of −0.47°C across all depths, but with less diel variability than for air temperature. Nevertheless, the soil cooling amount during periods of noon and dusk was greater than that during periods of night and dawn. Soil cooling amount during dusk was the highest of all periods, indicating a cumulative build-up of heat in the soil over the day. The highest 5 cm soil warming amount was −2.54°C in the afternoon (15:49) of 29 June (Fig. 7). Surface soil (5 cm) warming amount (−0.54°C) was consistently the lowest of the soil profile, but at other depths, soil warming amount also peaked at dusk from heat transfer processes requiring further modeling. The chances of realizing sustained warming at soil depths <30–50 cm by the design are not strong. Most soil warming occurred at the depth of 5 cm during noon and dusk periods with average warming amounts of −0.75°C and −0.70°C, respectively (Table 2). Since the site was flooded on 15 August, average soil warming amounts of 5 cm, 10 cm, 20 cm, and 30 cm increased by 59.3%, 57.2%, 51.2%, and 82.6%, respectively. Indeed, surface flooding influences soil temperature profiles throughout the experimental period, and trended toward stronger soil cooling potential when soils were at least slightly de-watered with water tables below −20 cm (Fig. 2).

Table 2. OTCs warming amount over separate diel periods.

Period	Air temp.	Soil temperature				
		5 cm	10 cm	20 cm	30 cm	mean
Night (21:00 to 3:00)	−0.27	−0.38	−0.39	−0.44	−0.51	−0.43
Dawn (3:00 to 9:00)	0.24	−0.33	−0.34	−0.38	−0.37	−0.36
Noon (9:00 to 15:00)	2.41	−0.75	−0.35	−0.49	−0.41	−0.50
Dusk (15:00 to 21:00)	0.83	−0.70	−0.44	−0.59	−0.62	−0.59
Daily	0.80	−0.54	−0.38	−0.47	−0.48	−0.47

3.4. Influence of OTCs warming on soil properties

In addition to temperature changes, other soil parameters were affected by the OTCs setup. Soil water content decreased significantly (p<0.01) at all depths for OTCs and control plots, with no soil depth variation within the OTCs (Fig. 8). This was unexpected. For example, no significant differences (p>0.05) were observed between water content at

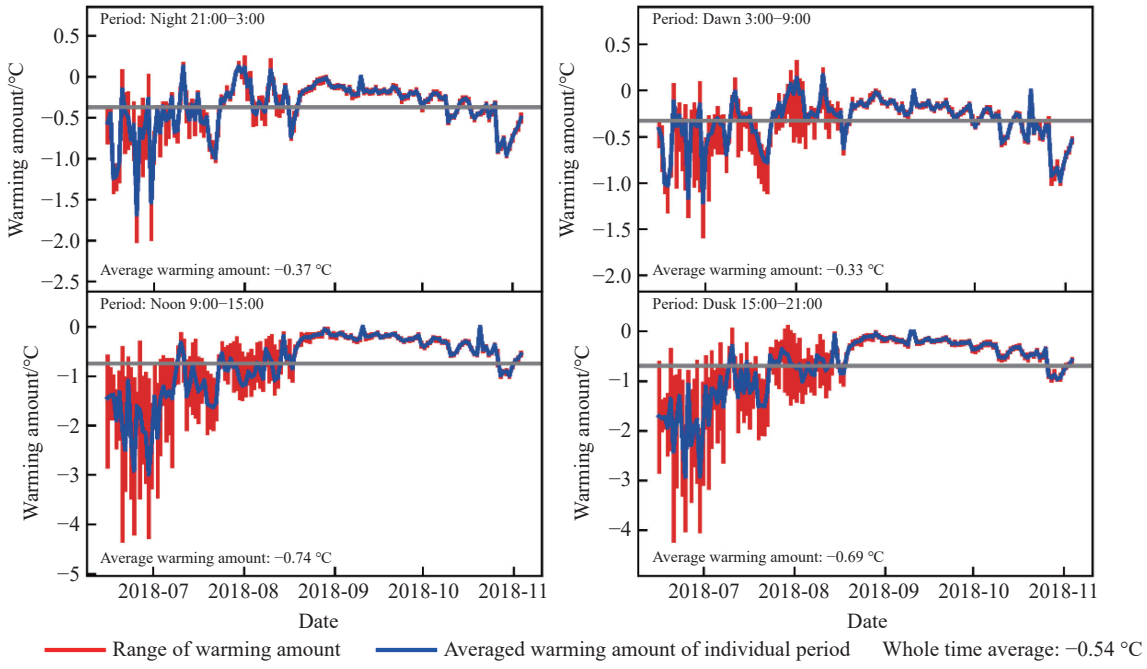

Fig. 7. OTCs warming amount of 5 cm depth soil temperatures over four diel periods. Periods were determined as night (21:00 to 3:00), morning (3:00 to 9:00), noon (9:00 to 15:00) and dawn (15:00 to 21:00). The red bars represent the warming amount range for a single day during a corresponding period. The blue lines represent the average warming amount of the corresponding period.

5 cm and 20 cm in the OTCs, which are depths that would be heavily influenced by the Phragmites root zone and therefore, a zone of purported water extraction as transpiration increases with OTCs warming. It was the same with water content at the depth of 10 cm and 30 cm. Among all profiles, the soil water content varied within a 10% volumetric ratio. The conductivity, however, increased with soil depth and reached the highest value of 3.0 dS/m at a depth of 30 cm, which represents a 30.3% decrease in conductivity at this depth in the OTCs versus controls (Fig. 8). Since no significant influence of warming amount occurred on soil conductivity at other depths, the authors implicate upper root zone (<30 cm depths) priming in concentrating soil ions to affect conductivity.

3.5. Influence of OTCs warming on Phragmites

In this study, the authors discovered a strong relationship between basal stem diameter and plant height for OTCs and control plots (Fig. 9). However, in the OTCs, *Phragmites* grew differently during the first year of warming. *Phragmites* inside the OTCs became thinner (smaller basal diameter) and taller. Based on the fitting curve, for identical basal stem diameters, the *Phragmites* inside the OTCs were 9.5% taller than those outside the OTCs.

Shoot numbers of *Phragmites* plants inside the OTCs of plot 4 and plot 6 were 18.3% and 9.0% higher, respectively, while for the other four plot comparisons (matched pairs, OTCs *vs.* control), control plots had higher shoot densities. In fact, the overall mean for shoot density was 235 shoot/m^2 for OTCs and 306 shoot/m^2 for control sites (Fig. 10). Overall, the OTCs warming experiment decreased *Phragmites* density by 71 shoot/m^2, accounting for a 23.2% change. In the control plots, the mean basal stem diameter of *Phragmites* plants was 3.83 mm, while it was 3.59 mm in the OTCs, which was 6.3% (p<0.01) thinner. In contrast, *Phragmites*' height inside the OTCs (173.9 cm) was significantly (p<0.01) higher than in the control plots (166.7 cm). The OTCs warming experiment increased *Phragmites*' height by 7.2 cm, which was equivalent to a 4.3% change. According to the authors' estimation, above-ground fresh biomass inside the OTCs was estimated to be 5179.9 g/m^2, while above-ground fresh biomass outside the OTCs was estimated to be 7841.6 g/m^2. Based on this estimation, the OTCs warming experiment significantly decreased plant productivity by 34% over this evaluation cycle (Fig. 10).

Along with warming, OTCs imposed additional short-term impact on the *Phragmites* (Fig. 11). Inside the OTCs, aphid attacks were periodically severe, and the aphids propagated on and crowded the *Phragmites* leaves, imposing an unknown influence on the plants. The magnitude of this circumstance, however, was restricted to the OTCs, also implicating experimental artefacts that will need sorting. In the control plots and surrounding environment, aphids were present and colonized *Phragmites*, but much fewer *Phragmites* were affected outside the OTCs. In addition, more *Phragmites* were lodging and twisted inside the OTCs, related to densities, with this specific activity barely observed outside the OTCs.

4. Discussion

4.1. Influencing factors of OTCs warming

No single parameter should be used to evaluate the structural warming capacity of OTCs. Thus, it was hard to compare the warming amounts of various OTCs. However, natural environmental warming will be a holistic ecosystem response in the future, and multiple environmental parameters will be altered simultaneously. For the OTCs, despite the observations that smaller open-top chamber areas relative to the height of the chamber give rise to higher experimental temperatures (Aronson EL et al., 2009; Marion GM et al., 1997), a large OTCs design (ca. 15 m^3 volume) were chosen. *Phragmites* is a large plant and produces complex vertical community structures needing to be represented. Large chambers produced appreciable warming influences on the air and soil.

The International Tundra Experiment (ITEX) recommended a hexagon open-top chamber for rigidity but with specific design elements. The top hole area of the ITEX OTCs was specified to be smaller than the base area

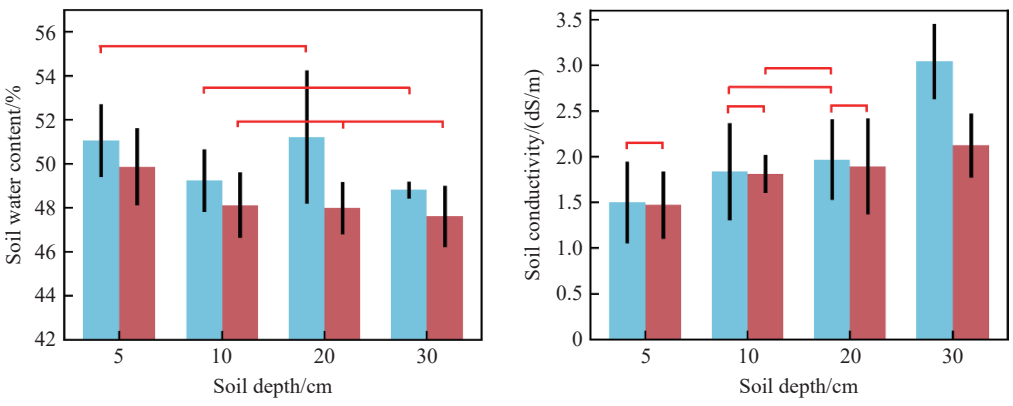

Fig. 8. Influence of OTCs warming on soil water content and soil conductivity at different soil depths. The blue bars indicate the traits of the control plots and the red bars indicate the traits of OTCs warming conditions. Bars represent standard deviations of the mean within each group to highlight the variability (*vs.* standard error). The horizontal red lines indicated no significant difference within each group.

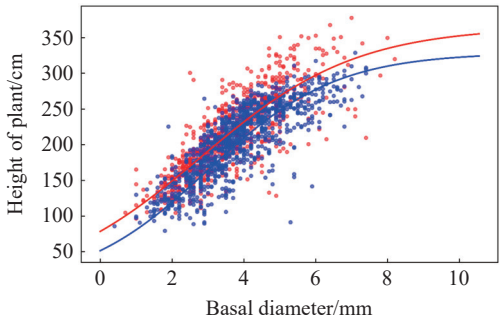

Fig. 9. Separated groups of the relationship between stem basal diameter and plant height. The red lines and symbols indicate plant traits inside the OTCs while the blue lines and symbols represent plant traits outside the OTCs (control). Lines represent least squares fitting, with a sigmoidal curve representing the best fit among those tested.

according to the "side dip angle" (Henry GHR and Molau U, 2010). In this study, the OTCs design was a 2.7 m high octagonal prism, covering 5.54 m^2, and the ratio of the height to the top hole area was 0.49/m. Wang JF and Wu QB (2013) reported two types of OTCs designs in the Qinghai-Tibet Plateau, and the chambers were 40 cm and 80 cm high with a base area of 0.9 m^2. The ratio, or side dip angle, was then calculated as 0.44/m and 0.89/m, respectively. So, the OTCs in the study were within the side dip angle range of smaller chambers, which may have contributed to the strong warming results. For the OTCs deployed in the Qinghai-Tibet Plateau, the closest site to this Yellow River Delta experiment, the 5 cm soil depth warming amount was 0.94°C, larger than the average 5 cm warming amount of 0.54°C. This indicated that OTCs warming amount had multiple controlling factors other than the structure of OTCs design, probably related to volume differences and the temperature and pressure stratification of large versus small volume OTCs.

Another OTCs design created by Cornelius C et al., 2015 set the side dip angle ratio to 0.89/m (top area 0.5625 m^2 and 0.5 m high), roughly twice this study, and the OTCs increased air temperature by 0.4°C to 0.9°C, which was comparable with this air warming amount of 0.80°C. Obviously, structural elements of the OTCs chambers are not the only criteria needed for warming. The OTCs warming are also strongly related to incident solar radiation (Fig. 5) and how that radiation is propagated through the top and side walls of OTCs structures. The rationale for setting side dip angles relates to how freely heat can escape, as was widely accepted, and OTCs warming amounts typically peak at noon on sunny days because radiation heating is high and heat escape is low (Hollister RD et al., 2006). Likewise, the results indicated a linear relationship between daily average net radiation and the OTCs warming amount, and as expected, the OTCs warming amount at noon was significantly higher than at night-time for multiple individual days (Figs. 4, 6) and daily averages (Table 2). Hollister RD et al., 2006 mentioned that higher plant coverage led to high warming amounts in their OTCs, and soil surface conditions such as soil type and inundation regime could also alter the thermal regime. Although the *Phragmites* did differ between these OTCs and control plots in terms of stem numbers, height, and biomass, the warming amount turbulence as well as another unpredictable impact of the OTCs design made it difficult to assign the consequence of the experiments to these observed results. However, soil flooding clearly affected the soil warming patterns (and would further influence VPD). Soil surfaces of OTCs were flooded after a 15 August rainfall event, and the average air warming amount dropped from 0.94°C to 0.68°C, which was equal to a 27.7% decline, while the relative humidity remain the same

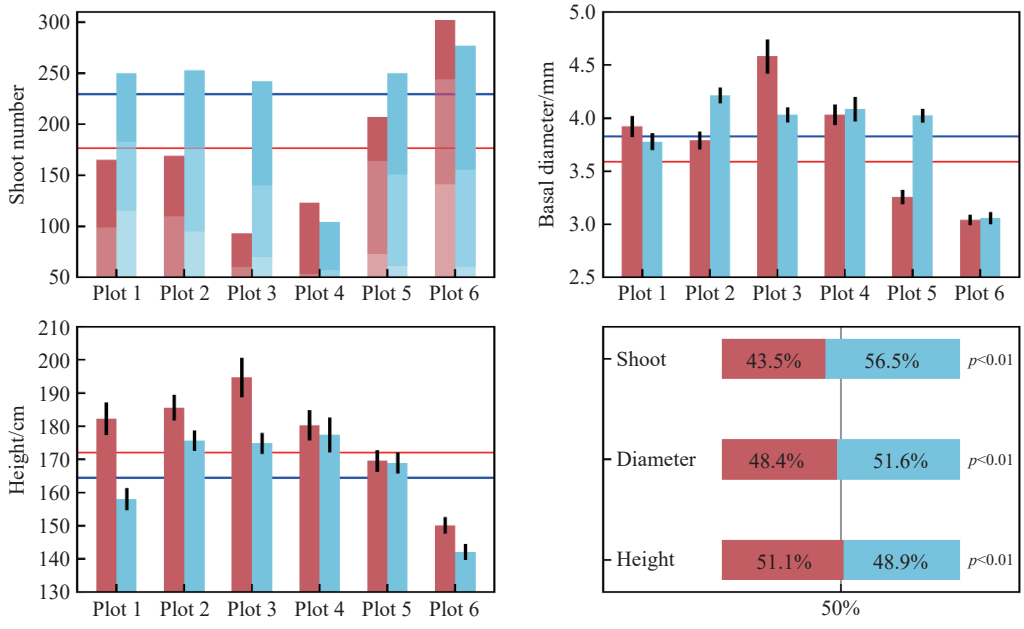

Fig. 10. Influence of OTCs warming on *Phragmites*' height and basal stem diameter. The color red represents OTCs warming conditions and the color blue represents non-warmed control plots. The stacked bars of the upper left pane indicate three selected quadrats. Bars represent standard errors of the mean.

after the same surface flooding event.

Wind speed was found to be negatively correlated with daily warming amount (Fig. 12; r^2=0.15, p<0.01), which is rarely mentioned in the literature. This is perhaps because the influence of wind speed is often theoretically more negligible compared to the influence of net radiation. Net radiation was indeed more positively correlated to daily warming amount (Fig. 12; r^2=0.20, p<0.01). The wind blows a lot in the Yellow River Delta. In fact, among the 141 days assessed, the wind was blowing over 2 m/s for 43.0% of the time, and over 4 m/s for 7.7 % of the time (Fig. 2). In summary, the warming amount of these OTCs were influenced most by net radiation and secondarily by wind speed while the influence of OTCs structure and soil surface condition (flooding) was correlative but applicable more to the structuring of soil temperature changes than the air temperature.

Occasional night-time air temperature depressions have been registered in past OTCs experiments (Marion GM et al., 1997). However, this phenomenon occurred during this experiment at a frequency higher than 60%. Indeed, normalized diel air temperature variation (Fig. 13) showed that the air temperature inside our OTCs was not occasionally

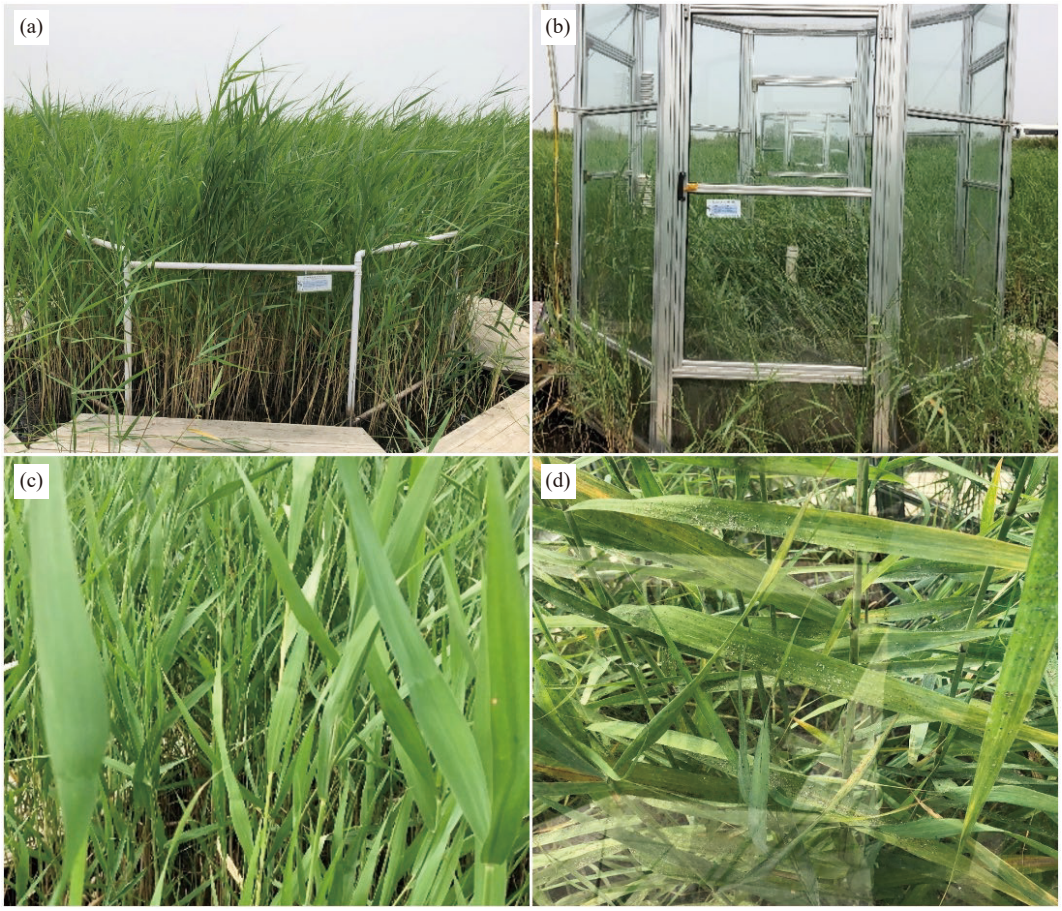

Fig. 11. Visual comparison of *Phragmites* inside and outside the OTCs. Common reeds grew normally and erect in control plots (a, c); whereas, lodging and aphid attacks occurred in the OTCs (b, d).

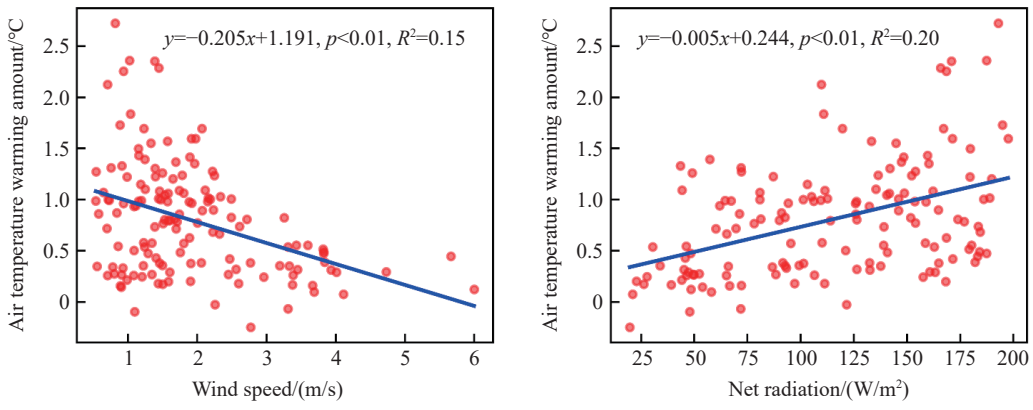

Fig. 12. Relationship between air temperature daily warming amount and its influencing factors of net radiation and wind speed.

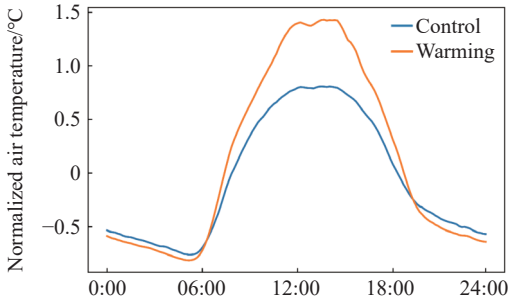

Fig. 13. Normalized air temperature inside and outside the OTCs. Within each observing day, the daily air temperature was linearly normalized by regulating the daily lowest air temperature as −1, the daily highest air temperature as 1, and the daily average air temperature as 0. All observed air temperature data from 14 June to 4 November were used.

but continuously lower than outside these OTCs during the night-time. By retaining heat, the authors expected that the air temperature inside the OTCs should be higher at nighttime than outside the OTCs, which conflicted with these findings. The climate data of night-time cooling processes from 5 July and 25–26 October were separated for detailed analyses. For both dates, soil temperatures inside the OTCs were lower than the outside temperatures at the same vertical positions, which indicated that there was continuous soil cooling during both nights. On 5 July, the air temperature difference between the high position (190 cm) and low position (100 cm) inside the OTCs kept decreasing along with simultaneous drops in net radiation. However, the high-position air temperature was consistently higher than the lower-position temperature (Fig. 14), providing evidence that the influence of soil warming on air temperature is limited, and the heat from the soil could hardly be transferred to the upward position; rather, warming is imposed from the top air toward the ground. The air inside the OTCs was more stable than outside air due to the much lower turbulence and sufficient wind buffering. Therefore, inside OTCs, an air-mixing device should probably be deployed and activated at night for mitigating the night-time cooling realized herein during subsequent deployments.

The low-position air temperature cooling started first, and then approximately 30 minutes later, the upper-position air temperature cooling started. This was consistent with the circumstances of the previous day. The cooling effect on the low position was larger than that on the high position except for after 4:00 on 26 October (Fig. 14). By then, the air temperature in the low position started to increase due to an upward transfer of warmth from the soil. Early on 26 October, net radiation dropped dramatically and enabled a temperature difference between the atmosphere and the soil surface, which was a factor for night-time cooling. Warmer air can contain more water vapor, and as the air temperature drops, dew points are reached, and water is deposited on leaf and chamber surfaces, releasing heat, which helps to maintain the temperature. This could explain why the cooling amount started to decrease as soon as vapor was deposited (RH drop)

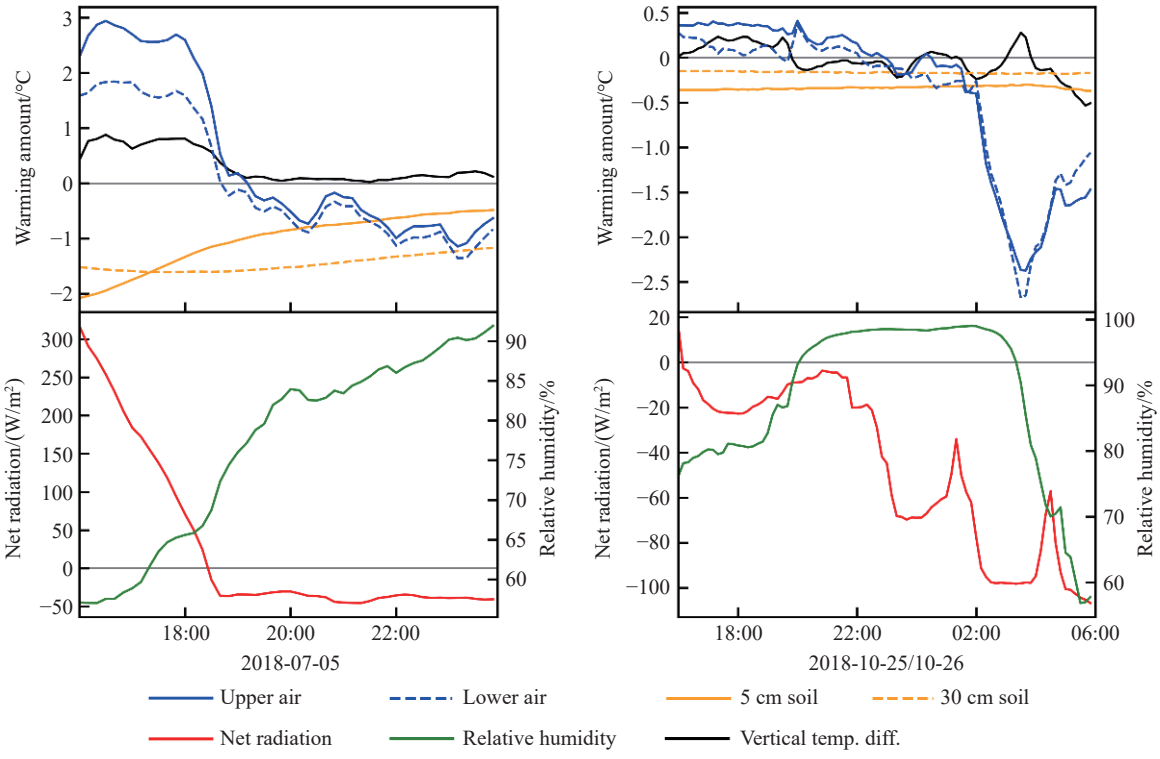

Fig. 14. Environmental factors contributing to OTCs' night-time cooling processes. In the upper panels, the black line represents the air temperature difference between the high position (190 cm) versus the low position (100 cm) inside OTCs. The red solid and dashed lines represent the warming amount of the high position and low position, respectively. The net radiation (NR) is represented by orange solid lines. In the lower panels, grey and black color indicate soil temperature responses at the soil depths of 5 cm and 30 cm, respectively, while the solid and dashed lines indicate the warming and control conditions, respectively. The relative humidity (RH) of inside OTCs air was marked as blue solid lines.

on 26 October. The greater moisture inside OTCs might also be contributing to insect infestations.

Based on the analysis, an explanation could be developed for the OTCs warming process (Fig. 15), which can then be used to improve future designs. OTCs influence inside air temperatures as inside air turbulence and mixing is also lowered. During the daytime, the highest warming amount occurred where solar radiation was most direct (plant canopy as represented by 190 cm sensors; bare soil surface), and the entire chamber is simultaneously warmed. During night-time, the OTCs in this study structure led to an air temperature depression except for the near-soil-surface part and the near-top-hole part. The circumstance indicated that the excessive heat obtained during daytime was trapped inside the soil instead of warming the entire OTCs.

4.2. Influence of OTCs warming on Phragmites

Stem elongation in graminoid plants depends on turgor maintenance in support of apical meristem cell division, while stem thickening is the result of cambial cell division (Pospišilová J et al., 1996). Due to the OTCs warming, more carbohydrates were allocated by *Phragmites* to elongate stems, as greater warming amounts were more often observed at higher vertical positions (190 cm *vs.* 100 cm), coinciding with the top of the active *Phragmites* canopy within our OTCs. *Phragmites* growing on the eastern edge of Chongming Island, China responded to similarly imposed OTCs warming by stretching their stems and increasing their shoot density, but this was done by imposing no influence on the basal stem diameter (Shi B et al., 2010). At this study site, an increase in basal stem diameter was observed and there was a decline in shoot density in the OTCs. This result from the study neither coincided with an average warming-imposed increase in plant productivity of 15%–22% from a previous meta-analysis (Rustad LE et al., 2001), nor with the data of Shi B et al., 2010, who also found that leaf, root, and total biomass increased by approximately 30%, 14%, and 24%, respectively, with experimental warming. These findings, on the other hand, indicated that plant productivity decreased by 34% with warming. The decrease in plant productivity was attributed to the decrease in shoot density in the study, which declined by 23.2%. The warming condition might also restrain plant sprouting and growth by transferring more biomass underground as the soil warming amount was more stable to the soil than to the air, and the authors have less understanding of the role that night-time cooling might have in reverse priming of day-time plant productivity in the OTCs. This needs further attention, as night-time cooling was more frequent in the OTCs versus other published accounts. The growth and productivity assessments are also so far, short-term spanning not quite a full growing season. Continuance of these studies in the Yellow River Delta and two additional sites in the Liaohe River Delta and coastal zone of Yancheng will reveal more details over time.

Crop lodging decreased plant productivity both in quality and quantity, and was undoubtedly related to reduced basal diameters in OTC-warmed *Phragmites*. Warming has previously been shown to trigger plant lodging in canola fields (Wu W and Ma BL, 2018). As the *Phragmites* shoots became taller and thinner, the risk of lodging increased, but the authors do not know whether lodging results from

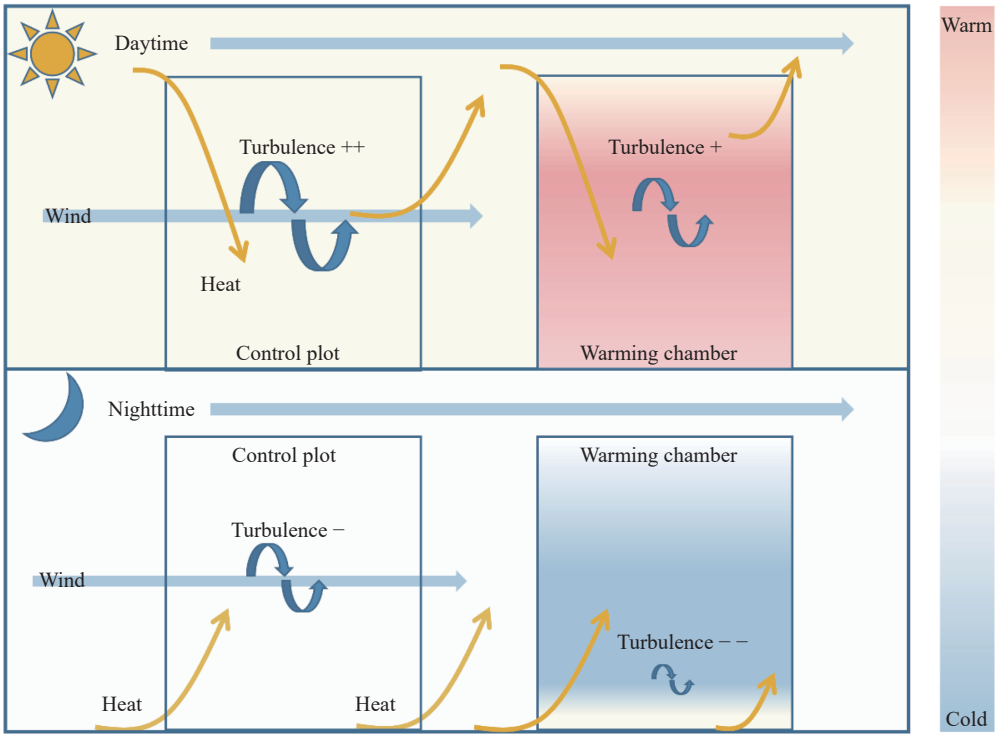

Fig. 15. Schematic explanation of OTCs warming as surmised from these experiments. The color bar demonstrates the relative temperature, and the orange arrows indicate the heat flow. Wind and turbulence were marked as blue arrows.

warming-induced growth responses of taller and thinner stems, or whether the shielding from wind reduces the need for *Phragmites* to produce thicker, more wind resilient stems. As the authors observed, reeds in all six OTCs suffered from the lodging of different extents (Fig. 11b); they became twisted and started to lean on a side of individual OTCs glass walls. Because of the lack of wind inside the OTCs, the shoot could grow no matter how slim the stem became. It was unexpected that the aphid attack inside the OTCs was so severe (Fig. 11d). Higher temperatures and moisture may have produced a benefit for the growing and breeding of aphids (Family *Aphididae*). Likewise, vastly reduced wind conditions inside OTCs made it easy for aphids to stay on leaves and congregate (Bale JS et al., 2002). However, it is important to note that there were previous reports of fewer herbivore insects from warming experiments (Adler LS et al., 2007; Burt MA et al., 2016), and lodging might even be one of the consequences of aphid attack (Pinthus MJ, 1974) rather than a warming growth response or wind buffering effect in *Phragmites*. Future procedures to isolate causes of specific growth effects might include control of future aphid outbreaks with insecticides or removal of glass panes from half of the warming chambers over specific periods to see if that influences growth responses of *Phragmites* and/or insect colonization patterns. Timing of panel removal will be a challenge since the authors don't know which are the most important periods for warming to be imposed, the early season, mid-season, or late season.

The response of plants to experimental warming is also species-dependent (de Valpine P and Harte J, 2001; Hollister RD et al., 2006). Plant density tends to increase in the grass- and sedge-dominated ecosystems with warming (Liu YZ et al., 2011; Mu JP et al., 2015). However, there was a 23.2% decline in plant density within these OTCs which were in agreement with Liu Y et al., 2012, such that trends might be inherently variable and situation-dependent. Reduced shoot numbers in *Phragmites* might be attributed to the role that early spring warming might have on shortening the sprouting period. The rapid accumulation of heat might stimulate plant growth earlier than the normal seasonal period and restrict bud development. As a result, the basal diameter might decrease while the stem becomes longer (as was observed) because there is more time for the *Phragmites* to grow. This might help to explain the biomass allocation caused by warming experiments only if the mechanism is physiological and relates to abiotic factors. While this current experiment was established too late in the growing season to discern OTCs versus control patterns of shoot initiation, the authors have the opportunity to test this hypothesis in future years.

Plant physiological response to OTCs warming would be expected to be different as soil hydrology and salinity change (Carey JC et al., 2016). Suseela V et al., 2015 found that the OTCs warming drove soil water loss and restricted ecosystem respiration; There was evidence that warming also induces soil conductivity increases at deeper soil depths to 30 cm. Measurements of soil and ecosystem CO_2 and CH_4 fluxes, including respiratory components, are on-going from the Yellow River Delta OTCs studies to provide further context. Plant production can be controlled by soil dehydration in a vascular-plant-dominated tundra (Day TA et al., 2010). Within the site, however, water was likely sufficient for most of the growing season except when the water level was below 30−50 cm for several days. The comparison between soil water contents inside and outside the OTCs indicates less than a 5% change in soil moisture content between the two treatments. No significant difference in soil conductivity change was found above 20 cm soil depth, but the authors are curious about the increased conductivity observed at 30 cm and in determining what those drivers might be with future studies. Continuous flooding in the last half of the growing season might also lower both inside OTCs and outside OTCs plant productivity (Warwick NWM and Brock MA, 2003). Although soil pore water salinity and soil water content determined plant productivity in *Phragmites* in the past studies (Sánchez E et al., 2015; Stefano RD et al., 2017), the local productivity of the Yellow River Delta Phragmites stock is less likely attributed to soil water content or salinity because both varied in extremely small ways across our study site.

The variation in plant response is likely to be related to the duration of warming exposure, which the authors intend to extend for multiple years. Some studies report no significant long-term responses of plants to warming in grasslands and wetlands (Baruah G et al., 2017; Hobbie SE and Chapin III FS, 1998), while the short-term OTCs warming exerted changes in plant physiological characteristics according to these results. Some studies concentrated on the acceleration of nutrient release and microbial rebalancing by warming conditions (Charles H and Dukes JS, 2009; Mcelroy DJ et al., 2015). As those plots were warmed for only one growing season, the biogeochemical cycle may not yet have been completely balanced or in sync with the new environment imposed by warming. The site remained dominated by *Phragmites*, and the community structure was not changed on a large scale. It is too early to estimate the long-term impact of OTCs warming on these *Phragmites* wetlands, but taking the first-year observation as a reference allows researchers to modify observing approaches, identify potential issues, and constrain artifacts moving forward with more comprehensive warming networks for multiple coastal wetland sites in China.

5. Conclusion

The customized OTCs were able to increase the inside air temperature up to 8.3°C during the daytime, and decrease it by as much as 2.5°C at night. During the growing season of 2018, the OTCs warmed inside air temperature by an average of 0.8°C and decreased the surface 5 cm soil temperature by an average of 0.54°C. Compared with wind speed, solar radiation was a slightly more dominant factor controlling the warming amount realized by the OTCs. The function of lowering internal turbulence generated by the OTCs structure

and the creation of a humidity-change depositional environment for atmospheric water resulted in night-time cooling, which offset the average warming amount as integration across full 24-hour diel cycles. The OTCs can decrease the soil water content of the entire soil profile to within a 10% volumetric ratio, which will also likely occur with increased environmental warming in the future, while it hardly changed soil conductivity above 20 cm depth. Soil conductivity was only influenced at a depth of 30 cm. The soil hydrology condition and pore water characteristics are resistant to OTCs warming experiments where the water supply is sufficient, making this coastal wetland a perfect field site for studying the influence of temperature change to ecosystem productivity.

The short-term OTCs warming experiment had multiple influences on the dominant plant *Phragmites*. For the same basal stem diameter, the Phragmites inside the OTCs were 9.5% taller than those outside the OTCs. Moreover, the OTCs warming experiment increases the average Phragmites height by 7.2 cm, or by 4.3%. The mean basal stem diameter in control plots was 3.83 mm, while it was 3.59 mm in the OTCs, which was 6.3% thinner. Corresponding plant density inside and outside the OTCs equated to 235 shoot/m^2 versus 306 shoot/m^2, respectively. Thus, the OTCs warming experiment decreased Phragmites density by 71 shoot/m^2 (or by 23.2%). According to biomass estimation, plant biomass was estimated to be reduced by 34% with warming, instead of increasing, which was at least partially related to the changes in individual plant traits and community changes such as pest damage and lodging within the warming chambers.

The results indicate that the influence of simulated warming experiments can be fairly successful from the perspective of the physical effect, but may also impose unpredictable effects on the wetland ecosystem that may or may not be a consequence of the environmental change we are intending to document, artifacts of these OTCs, or a combination of both. Honest reporting by purveyors of OTCs studies is necessary and is certainly assumed in past investigations. While the authors did not always have optimistic a priori projections that warmed *Phragmites* would fix more atmospheric carbon, the authors did assume that the OTCs design and corresponding warming would be less complex than the authors were able to describe by the intense sensor network. Thus, the variation of plant productivity or carbon input was attributed to the multidimensional influence of the OTCs; measuring one or even a few dimensions only would be to shield the entire story related to OTCs experimentation. Assessment of OTCs warming patterns should be carefully made instead of simply demonstrating the average warming amount, and artifacts need specific detailing to use experimental responses appropriately within future modeling projections.

CRediT authorship contribution statement

Si-yuan Ye, Xue-yang Yu, Ken W. Krauss, Samantha K. Chapman, and Hans Brix conceived of the presented idea. Xue-yang Yu, Li-xin Pei, and Liu-juan Xie experimented. All authors discussed the results, provided critical feedback, and contributed to the final manuscript.

Declaration of competing interest

The authors declare no conflicts of interest.

Acknowledgment

This study was jointly funded by the Marine S&T Fund of Shandong Province for the Pilot National Laboratory for Marine Science and Technology (Qingdao)(2022QNLM 040003-3), the National Key R&D Program of China (2016YFE0109600), National Natural Science Foundation of China (U22A20558, 41240022, 41876057, 40872167, 41602143), China Geological Survey (1212010611402, GZH201200503, and DD20160144), and by in-kind support from the Land Carbon Program and Land Change Science R&D Program of the United States Geological Survey.

References

Adler LS, Valpine PD, Harte J, Call J. 2007. Effects of long-term experimental warming on Aphid density in the field. Journal of the Kansas Entomological Society, 80(2), 156–168. doi: 10.2317/0022-8567(2007)80[156:EOLEWO]2.0.CO;2.

Aronson EL, Mcnulty SG, Sun G, Sun JX, Zhou GS. 2009. Appropriate experimental ecosystem warming methods by ecosystem, objective, and practicality. Agricultural and Forest Meteorology, 149(11), 1791–1799. doi: 10.1016/j.agrformet.2009.06.007.

Baldwin AH, Jensen K. 2014. Warming increases plant biomass and reduces diversity across continents, latitudes, and species migration scenarios in experimental wetland communities. Global Change Biology, 20(3), 835–850. doi: 10.1111/gcb.12378.

Bale JS, Masters GJ, Hodkinson ID, Awmack C, Bezemer TM, Brown VK, Butterfield J, Buse A, Coulson JC, Farrar J, Good JEG, Harrington R, Hartley S, Jones TH, Lindroth RL, Press MC, Symrnioudis I, Watt AD, Whittaker JB. 2002. Herbivory in global climate change research: direct effects of rising temperature on insect herbivores. Global Change Biology, 8(1), 1–16. doi: 10.1046/j.1365-2486.2002.00451.x.

Baruah G, Molau U, Bai Y, Alatalo JM. 2017. Community and species-specific responses of plant traits to 23 years of experimental warming across subarctic tundra plant communities. Scientific Reports, 7, 2571. doi: 10.1038/s41598-017-02595-2.

Bondlamberty B, Thomson A. 2010. Temperature-associated increases in the global soil respiration record. Nature, 464(7288), 579–582. doi: 10.1038/nature08930.

Burt MA, Dunn RR, Nichols LM, Sanders NJ. 2016. Interactions in a warmer world: Effects of experimental warming, conspecific density, and herbivory on seedling dynamics. Ecosphere, 5(1), 1–12. doi: 10.1890/ES13-00198.1.

Carey JC, Kroeger KD, Zafari B, Tang JW. 2018. Passive experimental warming decouples air and sediment temperatures in a salt marsh. Limnology and Oceanography: Methods, 16, 640–648. doi: 10.1002/lom3.10270.

Carey JC, Tang J, Templer PH, Kroeger KD, Crowther TW, Burton AJ, Dukes JS, Emmett B, Frey SD, Heskel MA. 2016. Temperature response of soil respiration largely unaltered with experimental warming. Proceedings of the National Academy of Sciences of the

United States of America, 113(48), 13797. doi: 10.1073/pnas.1605365113.

Charles H, Dukes JS. 2009. Effects of warming and altered precipitation on plant and nutrient dynamics of a New England Salt Marsh. Ecological Applications, 19(7), 1758–1773. doi: 10.1890/08-0172.1.

Chen J, Luo YQ, Xia JY, Zheng S, Jiang LF, Niu SL, Zhou XH, Cao JJ. 2016. Differential responses of ecosystem respiration components to experimental warming in a meadow grassland on the Tibetan Plateau. Agricultural and Forest Meteorology, 220, 21–29. doi: 10.1016/j.agrformet.2016.01.010.

Cornelius C, Heinichen J, Drösler M, Menzel A. 2015. Impacts of temperature and water table manipulation on grassland phenology. Applied Vegetation Science, 17(4), 625–635. doi: 10.1111/avsc.12105.

Crowther TW, Toddbrown KEO, Rowe CW, Wieder WR, Carey JC, Machmuller MB, Snoek BL, Fang S, Zhou G, Allison SD. 2016. Quantifying global soil carbon losses in response to warming. Nature, 540(7631), 104–108. doi: 10.1038/nature20150.

Day TA, Ruhland CT, Xiong FS. 2010. Warming increases aboveground plant biomass and C stocks in vascular-plant-dominated Antarctic tundra. Global Change Biology, 14(8), 1827–1843. doi: 10.1111/j.1365-2486.2008.01623.x.

Deegan LA, Johnson DS, Warren RS, Peterson BJ, Fleeger JW, Fagherazzi S, Wollheim WM. 2012. Coastal eutrophication as a driver of salt marsh loss. Nature, 490(7420), 388–392. doi: 10.1038/nature11533.

de Valpine P, Harte J. 2001. Plant responses to experimental warming in a montane meadow. Ecology, 82(3), 637–648. doi: 10.1890/0012-9658(2001)082[0637:PRTEWI]2.0.CO;2.

Ding YR, Ye SY, Zhao QS. 2012. Nutrients and carbon sequestration in the newly created wetlands of the Yellow River Delta. Geological Review, 58(1), 183–189 (in Chinese with English abstract). doi: 10.16509/j.georeview.2012.01.009.

Edith B, Li SL, Xu WH, Li W, Dai WW, Jiang P. 2013. A meta-analysis of experimental warming effects on terrestrial nitrogen pools and dynamics. New Phytologist, 199(2), 441–451. doi: 10.1111/nph.12252.

Fu G, Zhang XZ, Zhang YJ, Shi PL, Li YL, Zhou YT, Yang PW, Shen ZX. 2013. Experimental warming does not enhance gross primary production and above-ground biomass in the alpine meadow of Tibet. Journal of Applied Remote Sensing, 7(7), 6451–6465. doi: 10.1117/1.JRS.7.073505.

Grogan P, Chapin III FS. 2000. Initial effects of experimental warming on above and belowground components of net ecosystem CO_2 exchange in arctic tundra. Oecologia, 125(4), 512–520. doi: 10.1007/s004420000490.

Hawkins E, Ortega P, Suckling E, Schurer A, Hegerl G, Jones P, Joshi M, Osborn TJ, Masson-Delmotte V, Mignot J, Thorne P, Oldenborgh GJ. 2017. Estimating changes in global temperature since the Preindustrial Period. Bulletin of the American Meteorological Society, 98(9), 1841–1856. doi: 10.1175/bams-d-16-0007.1.

Henry GHR, Molau U. 2010. Tundra plants and climate change: The International Tundra Experiment (ITEX). Global Change Biology, 3(S1), 1–9. doi: 10.1111/j.1365-2486.1997.gcb132.x.

Hobbie SE, Chapin III FS. 1998. The response of tundra plant biomass, aboveground production, nitrogen, and CO_2 flux to experimental warming. Ecology, 79(5), 1526–1544. doi: 10.1890/0012-9658(1998)079[1526:TROTPB]2.0.CO;2.

Hollister RD, Webber PJ, Nelson FE, Tweedie CE. 2006. Soil thaw and temperature response to air warming varies by plant community: Results from and open-top chamber experiment in northern Alaska. Arctic Antarctic and Alpine Research, 38(2), 206–215. doi: 10.1657/1523-0430(2006)38[206:STATRT]2.0.CO;2.

IPCC. 2013. Climate Change 2013: The Physical Science Basis. Contribution of Working Group I to the Fifth Assessment Report of the Intergovernmental Panel on Climate Change. Cambridge, Cambridge University Press, 1535.

IPCC. 2022. Global Warming of 1.5°C: IPCC Special Report on Impacts of Global Warming of 1.5°C above Pre-industrial Levels in Context of Strengthening Response to Climate Change, Sustainable Development, and Efforts to Eradicate Poverty. Cambridge, Cambridge University Press. doi: 10.1017/9781009157940.

King G, Adamsen A. 1992. Effects of temperature on methane consumption in a forest soil and in pure cultures of the methanotroph Methylomonas rubra. Applied and Environmental Microbiology, 58(9), 2758–2763. doi: 10.1128/aem.58.9.2758-2763.1992.

Körner C, Basler D. 2010. Plant science. Phenology under global warming. Science, 327(5972), 1461–1462. doi: 10.1126/science.1186473.

Li JW, Ziegler SE, Lane CS, Billings SA. 2015. Warming-enhanced preferential microbial mineralization of humified boreal forest soil organic matter: Interpretation of soil profiles along a climate transect using laboratory incubations. Journal of Geophysical Research Biogeosciences, 117(G2), 502–504. doi: 10.1029/2011JG001769.

Liu J, Ye SY, Yuan HM, Ding XG, Zhao GM, Yang SX, He L, Wang J, Pei SF, Huang XY. 2018. Metal pollution across the upper delta plain wetlands and its adjacent shallow sea wetland, northeast of China: Implications for the filtration functions of wetlands. Environmental Science and Pollution Research, 25(6), 5934–5949. doi: 10.1007/s11356-017-0912-3.

Liu Y, Mu J, Niklas KJ, Li G, Sun S. 2012. Global warming reduces plant reproductive output for temperate multi-inflorescence species on the Tibetan plateau. New Phytologist, 195(2), 427–436. doi: 10.1111/j.1469-8137.2012.04178.x.

Liu YZ, Reich PB, Li GY, Sun SC. 2011. Shifting phenology and abundance under experimental warming alters trophic relationships and plant reproductive capacity. Ecology, 92(6), 1201–1208. doi: 10.1890/10-2060.1.

Macdonald JA, Fowler D, Hargreaves KJ, Skiba U, Leith ID, Murray MB. 1998. Methane emission rates from a northern wetland: Response to temperature, water table and transport. Atmospheric Environment, 32(19), 3219–3227. doi: 10.1016/S1352-2310(97)00464-0.

Marion GM, Ghr H, Freckman DW, Johnstone J, Jones G, Jones MH, Lévesque E, Molau U, Mølgaard P, Parsons AN. 1997. Open-top designs for manipulating field temperature in high-latitude ecosystems. Global Change Biology, 3(S1), 20–32. doi: 10.1111/j.1365-2486.1997.gcb136.x.

Mcelroy DJ, O 'Gorman EJ, Schneider FD, Hetjens H, Merrer PL, Coleman RA, Emmerson M. 2015. Size-balanced community reorganization in response to nutrients and warming. Global Change Biology, 21(11), 3971–3981. doi: 10.1111/gcb.13019.

Meng L, Roulet N, Zhuang QL, Christensen TR, Frolking S. 2016. Focus on the impact of climate change on wetland ecosystems and carbon dynamics. Environmental Research Letters, 11(10), 100201. doi: 10.1088/1748-9326/11/10/100201.

Mozdzer TJ, Caplan JS. 2018. Complementary responses of morphology and physiology enhance the stand-scale production of a model invasive species under elevated CO_2 and nitrogen. Functional Ecology, 32(7), 1784–1796. doi: 10.1111/1365-2435.13106.

Mu JP, Peng YH, Xi XQ, Wu XW, Li GY, Niklas KJ, Sun SC. 2015. Artificial asymmetric warming reduces nectar yield in a Tibetan alpine species of Asteraceae. Annals of Botany, 116(6), 899–906. doi: 10.1093/aob/mcv042.

Perillo GME, Wolanski E, Cahoon D, Brinson M. 2009. Coastal Wetlands: An Integrated Ecosystem Approach. Elsevier, Amsterdam, 941.

Pinthus MJ. 1974. Lodging in wheat, barley, and oats: The phenomenon, its causes, and preventive measures. Advances in Agronomy, 25, 209–263. doi: 10.1016/S0065-2113(08)60782-8.

Pospišilová J, Mohr H, Schopfer P. 1996. Plant physiology. Biologia Plantarum, 38, 458. doi: 10.1007/BF02896680.

Rätsep M, Muru R, Freiberg A. 2018. High temperature limit of photosynthetic excitons. Nature Communications, 9(1), 99. doi: 10.1038/s41467-017-02544-7.

Romero-Olivares AL, Allison SD, Treseder KK. 2017. Soil microbes and their response to experimental warming over time: A meta-analysis of field studies. Soil Biology and Biochemistry, 107, 32–40. doi: 10.1016/j.soilbio.2016.12.026.

Rouse WR, Carlson DW, Weick EJ. 1992. Impacts of summer warming on the energy and water balance of wetland tundra. Climatic Change, 22(4), 305–326. doi: 10.1007/BF00142431.

Rustad LE, Campbell JL, Marion GM, Norby RJ, Mitchell MJ, Hartley AE, Cornelissen JHC, Gurevitch J, GCTE-NEWS. 2001. A meta-analysis of the response of soil respiration, net nitrogen mineralization, and aboveground plant growth to experimental ecosystem warming. Oecologia, 126(4), 543–562. doi: 10.1007/s004420000544.

Sánchez E, Scordia D, Lino G, Arias C, Cosentino SL, Nogués S, Lee DK, Shinners K, Finnan J, Tyner W. 2015. Salinity and water stress effects on biomass production in different *Arundo donax* L. clones. Bioenergy Research, 8(4), 1461–1479. doi: 10.1007/s12155-015-9652-8.

Shi B, Ma JY, Wang KY, Gong JN, Zhang C, Liu WH. 2010. Effects of atmospheric elevated temperature on the growth, reproduction and biomass allocation of reclamation Phragmites australis in east beach of Chongming Island. Resources and Environment in the Yangtze Basin, 19(4), 383–388 (in Chinese with English abstract).

Stefano RD, Cappetta E, Guida G, Mistretta C, Caruso G, Giorio P, Albrizio R, Tucci M. 2017. Screening of giant reed (*Arundo donax* L) ecotypes for biomass production under salt stress. Plant Biosystems, 152(5), 1–7. doi: 10.1080/11263504.2017.1362059.

Sun SQ, Peng L, Wang GX, Wu YH, Zhou J, Bing HJ, Yu D, Luo J. 2013. An improved open-top chamber warming system for global change research. Silva Fennica, 47(2), 250–254. doi: 10.14214/sf.960.

Suseela V, Conant RT, Wallenstein MD, Dukes JS. 2015. Effects of soil moisture on the temperature sensitivity of heterotrophic respiration vary seasonally in an old-field climate change experiment. Global Change Biology, 18(1), 336–348. doi: 10.1111/j.1365-2486.2011.02516.x.

Wang JF, Wu QB. 2013. Impact of experimental warming on soil temperature and moisture of the shallow active layer of wet meadows on the Qinghai-Tibet Plateau. Cold Regions Science and Technology, 90–91. doi: 10.1016/j.coldregions.2013.03.005.

Warwick NWM, Brock MA. 2003. Plant reproduction in temporary wetlands: The effects of seasonal timing, depth, and duration of flooding. Aquatic Botany, 77(2), 153–167. doi: 10.1016/S0304-3770(03)00102-5.

Wookey PA, Parsons AN, Welker JM, Potter JA, Callaghan TV, Lee JA. 1993. Comparative responses of phenology and reproductive development to simulated environmental change in sub-arctic and high arctic plants. Oikos, 67(3), 490–502. doi: 10.2307/3545361.

Wu W, Ma BL. 2018. Assessment of canola crop lodging under elevated temperatures for adaptation to climate change. Agricultural and Forest Meteorology, 248, 329–338. doi: 10.1016/j.agrformet.2017.09.017.

Xu YY, Ramanathan V. 2012. Latitudinally asymmetric response of global surface temperature: Implications for regional climate change. Geophysical Research Letters, 39(13), 13706. doi: 10.1029/2012GL052116.

Ye SY, Krauss KW, Brix H, Wei MJ, Olsson L, Yu XY, Ma XY, Wang J, Yuan HM, Zhao GM. 2016. Inter-annual variability of area-scaled gaseous carbon emissions from wetland soils in the Liaohe Delta, China. PLoS ONE, 11(8), e0160612. doi: 10.1371/journal.pone.0160612.

Yu JB, Li YZ, Han GX, Zhou D, Fu YQ, Guan B, Wang GM, Ning K, Wu HF, Wang JH. 2014. The spatial distribution characteristics of soil salinity in coastal zone of the Yellow River Delta. Environmental Earth Sciences, 72(2), 589–599. doi: 10.1007/s12665-013-2980-0.

Yu XY, Ye SY. 2020. The universal applicability of logistic curve in simulating ecosystem carbon dynamic. China Geology, 3(2), 292–298. doi: 10.31035/cg2020029.

Zhang ZS, Xue ZS, Lu XG, Jiang M, Mao DH, Huo LL. 2017. Warming in spring and summer lessens carbon accumulation over the past century in temperate wetlands of Northeast China. Wetlands, 37(5), 829–836. doi: 10.1007/s13157-017-0915-3.

Zhou YM, Hagedorn F, Zhou CL, Jiang XJ, Wang XX, Li MH. 2016. Experimental warming of a mountain tundra increases soil CO_2 effluxes and enhances CH_4 and N_2O uptake at Changbai Mountain, China. Scientific Reports, 6(1), 21108. doi: 10.1038/srep21108.

Zhu JT, Zhang YJ, Jiang L. 2017. Experimental warming drives a seasonal shift of ecosystem carbon exchange in Tibetan alpine meadow. Agricultural and Forest Meteorology, 233, 242–249. doi: 10.1016/j.agrformet.2016.12.005.